

Stress waves transmission from railway track over geogrid reinforced ballast underlain by clay

Mohammed Y. Fattah^{*}, Mahmood R. Mahmood^a and Mohammed F. Aswad^b

Civil Engineering Department, University of Technology, Baghdad, Iraq

(Received April 13, 2019, Revised November 6, 2019, Accepted March 19, 2022)

Abstract. Extensive laboratory tests were conducted to investigate the effect of load amplitude, geogrid position, and number of geogrid layers, thickness of ballast layer and clay stiffness on behavior of reinforced ballast layer and induced strains in geogrid. A half full-scale railway was constructed for carrying out the tests, the model consists of two rails 800 mm in length with three wooden sleepers (900 mm × 10 mm × 10 mm). The ballast was overlying 500 mm thickness clay in two states, soft and stiff state. Laboratory tests were conducted to investigate the response of the ballast and the clay layers where the ballast was reinforced by a geogrid. Settlement in ballast and clay, soil pressure and pore water pressure induced in the clay were measured in reinforced and unreinforced ballast cases. It was concluded that the effect of frequency on the settlement ratio is almost constant after 500 cycles. This is due to that the total settlement after 500 cycles, almost reached its peak value, which means that the ballast particles become very close to each other, so the frequency is less effective for high contact particles forces. The average maximum vertical stress and pore water pressure increased with frequency.

Keywords: ballast; clay; frequency; geogrid reinforcement; pore water pressure

1. Introduction

Railway ballast gradually evolved from the early practice of simply using locally available gravel to the use of coarse and open-graded hard crushed rock. Appreciation for ballast and other components of the track substructure has grown throughout the history of the railway industry. The track superstructure includes the main load-supporting elements of the track that react and transfer train load to the track substructure. The superstructure includes the rail, tie (sleeper), and fastening system that work together to support train loading by reducing the large stresses at the wheel–rail interface to levels that are tolerable for the substructure layers.

The superstructure is required to resist both vertical and lateral loads with only small elastic and permanent deformation.

The thickness of the ballast layer should be specified based on the structural capacity of the track to ensure that it can withstand and distribute the applied train loading at a stress level that will not deform the subgrade over the expected life of the track. Ballast compaction is essential to

*Corresponding author, Ph.D., Professor, E-mail: myf_1968@yahoo.com

^a Professor

^b Assistant Professor

provide lateral track resistance. Although ballasted track is normally very stable with a considerable lateral strength reserve to resist imposed stresses, when ballast is newly placed or if it has been disturbed by maintenance (tamping or tie replacement), lateral resistance of the track may only be half of its value compared to when it is compacted. Resumed traffic following the maintenance will lead to gradual ballast recompaction and eventual restoration of its lateral strength and track buckling resistance (Li *et al.* 2016).

Reinforcement conventionally placed at strategical position in earth structures in the places where the maximum plastic tensile strain, to minimize that strain by carrying out tensile stress by itself. This requires good interaction to transmit stress from granular soils to the reinforcement. If geogrid reinforcement is used, this demands high interlock. The reinforcement resists the base material extension strains with the provided confinement resulting from the tensile strength of the geogrid.

Track settlement occurs after long-term service. According to Selig and Waters (1994), ballast contributes the most to track settlement, even though one of the functions of ballast is to restrain track geometry. Excessive settlement can cause poor passenger comfort, speed restriction, and potential derailment.

Despite the problems associated with ballast, ballast is still a preferable choice for substructure material over other alternatives such as concrete slabs or asphalt. This is because ballast provides less stiff support which is an important factor in case of differential settlement or subgrade failure, ballast is more economical, produces less noise (Profillidis 2000) contributes in damping impact wheel load and railway track vibration, distributes transmitted stresses evenly, reduces the settlements and provides a good base layer under low confining pressures. However, there are many cases where using ballast individually may not be sufficient because of subgrade layer weakness.

Vibration would not have been an unfamiliar occurrence in the past. Even during the age of horse-driven carriages on cobblestone streets, strong complaints of vibrations arose from occupants of buildings along the route. However, no convincing explanations were made in that period. Therefore, for a long period, train loads have been believed to be reasonably assumed as quasi-static moving loads. Krylov (1995) considered that a train will encounter the “sound barrier” (critical speed) when reaching the velocity of Rayleigh surface waves propagating in the ground. The critical condition was explained as resonance between the moving train and the Rayleigh wave of the subgrade soil (Gao 2013).

Sowmiya *et al.* (2011) studied geosynthetic reinforced railway tracks model using ABAQUS 6.9 with different sub ballast thicknesses and compared with unreinforced section. The results showed that the reinforcement can be used to improve the performance of railway tracks on clayey subgrade. The study showed that the reinforcement between sub ballast and subgrade, between ballast and sub ballast and the reinforcement at both the interfaces reduce induced vertical stresses and displacements significantly. The conclusion of the study was that to reduce the maintenance cost and to reduce the shear failure, the reinforcement between sub ballast and subgrade, between ballast and sub ballast and the reinforcement at both the interfaces are the best options.

Nguyen *et al.* (2011) worked to develop the most adequate and efficient models for calculation of dynamic traffic load effects on railways track infrastructure, and then evaluate the dynamic effect on the ballast track settlement, using a ballast track settlement prediction model, which consists of the vehicle/track dynamic model previously selected and a track settlement law. The calculations were based on dynamic finite element models with direct time integration, contact between wheel and rail and interaction with railway cars. The results obtained included the track

irregularity growth and the contact force in the final interaction of numerical simulation. They included that an increase of train speed will produce higher contact forces between the wheel and the rail, and will produce larger deflections in the ballast and a larger settlement will be obtained.

Leshchinsky and Ling (2013), carried out a numerical modeling using finite element analysis according to experimental results of large-scale laboratory tests of geocell reinforced ballast embankments for confinement. The study was to explore (the geocell confinement effects on ballasted embankments resting on soft subgrade, different ballast stiffnesses, and varying stiffness of reinforcement). From the results, it was found that geocell confinement has a significant benefit on a wide range of subgrade stiffness. The effect of the confined ballast is distributing stresses more uniformly to the subgrade, which can provide higher bearing capacities and less settlement.

Hayano *et al.* (2013) studied the effects of ballast thickness and tie-tamper repair on the settlement characteristics of ballasted tracks by conducting a series of cyclic loading tests on model grounds. Results suggested that the 250 mm ballast thickness currently adopted as the standard design is ineffective for minimizing settlement that occurs when the nonlinearity of roadbed compressibility is relatively moderate. Moreover, characteristics of the initial settlement process are altered significantly after tie-tamper implementation, although the degree of gradual subsidence undergoes minimal change regardless of ballast thickness and roadbed type.

Wayne *et al.* (2013) conducted a controlled field study in Weirton, West Virginia, USA; to evaluate performance of a geogrid stabilized unpaved aggregate base overlying relatively weak and non-uniform subgrade soils. The results showed that the horizontal pressures within the subgrade created by both the static and live loading conditions were significantly reduced by using the geogrid. Also results confirmed that the geogrid improved aggregate confinement and interaction, leading to enhanced structural performance of the unpaved aggregate base.

Chen (2013) presented an evaluation of the behavior of geogrid-reinforced railway ballast. Experimental large box pull-out tests were conducted to examine the key parameters influencing the interaction between ballast and the geogrid. The experimental results demonstrated that the triaxial geogrid with triangular apertures outperforms the biaxial geogrid with square apertures and the geogrid aperture size is more influential than rib profile and junction profile. The discrete element method (DEM) has then been used to model the interaction between ballast and geogrid by simulating large box pull-out tests and comparing with experimental results. The DEM simulation results have been shown to provide good predictions of the pull-out resistance and reveal the distribution of contact forces in the geogrid-reinforced ballast system.

A three dimensional numerical model capable of modeling the propagation and transmission of ground vibration in the vicinity of high speed railways was produced by Connolly *et al.* (2013). It was used to investigate the effect of embankment constituent material on ground borne vibration levels at various distances from the track. The model is a time domain explicit, dynamic finite element model capable of simulating non-linear excitation mechanisms. The entire model, including the wheel/rail interface is fully coupled. To account for the unbounded nature of the soil structure an absorbing boundary condition (infinite element) is placed at the truncated interfaces. Lastly, quasi-static and dynamic excitation mechanisms of the vehicle locomotives were described using a multi-body approach which is fully coupled to the track using non-linear Hertzian contact theory. The resulting model was verified using experimental ground borne vibration data from high speed trains, gathered through field trials. It was then used to investigate the role of embankments in the transmission of vibration. It was found that soft embankments exhibit large deflections and act as a waveguide for railway vibrations which are trapped within the structure. This results in increased vibration levels both inside the embankment and in the surrounding soil.

In contrast it is found that embankments formed from stiffer material reduce vibrations in the near and far fields.

Aikawa (2015) carried out a research on the dynamic responses measured on a commercial line with ballasted track using sensing sleepers and sensing stones both of which were developed for the purpose of gaining new knowledge that will contribute to measures against track deterioration and effective track maintenance. The results of the spectral analysis showed that the rigid body vibration mode of sleepers is in a frequency range lower than 100 Hz and also revealed that the elastic vibration modes of ballast layers are in a frequency range as wide as 400-800 Hz. This series of analyses suggested the possibility that the dynamic load of a passing train is hard to damp, affected by its resonance.

Fattah *et al.* (2017) conducted laboratory tests to investigate the effect of load amplitude, load frequency, on the behavior of reinforced and unreinforced ballast layer. A half full-scale railway was constructed for carrying out the tests, which consists of two rails 800 mm in length with three wooden sleepers (900 mm × 90 mm × 90 mm). The ballast was overlying 500 mm thickness clay. It was concluded that the amount of settlement increased with increasing the simulated train load amplitude, there is a sharp increase in settlement up to the cycle 500 and after that, there is a gradual increase to level out between, 2500 to 4500 cycles depending on the used frequency. There is a little increase in the induced settlement when the load amplitude increased from 0.5 to 1 ton but it is higher when the load amplitude increased to 2 ton, the increasing amount in settlement depends on the geogrid existence and the other studied parameters. For unreinforced case, it was observed that the experimental results at the beginning show higher readings than the numerical ones, but after a number of cycles ranging from 750 to 2500 cycles the numerical results show higher readings. In a later study, Fattah *et al.* (2019) concluded that the amount of settlement increased as the simulated train load amplitude increased, and there was a sharp increase in settlement up to cycle 500. After that, there was a gradual increase that leveled out between, 2500 to 4500 cycles depending on the frequency used. There was a slight increase in the induced settlement when the load amplitude increased from 0.5 to 1 ton but it was higher when the load amplitude increased to 2 tons. The increased amount in settlement depended on the existence of the geogrid and other parameters studied. The transmitted average vertical stress for ballast thicknesses of 30 cm and 40 cm increased as the load amplitude increased, regardless of the ballast reinforcement for both soft and stiff clay. The position of the geogrid had no significant effect on the transmitted stresses. The value of the soil pressure and pore water pressure on ballast thicknesses of 20 cm was higher than for 30 cm and 40 cm thicknesses. This meant that the ballast attenuated the induced waves. The soil pressure and pore water pressure for reinforced and unreinforced ballast was higher in stiff clay than in soft clay.

To estimate the effect of differential subgrade settlement on the mechanical behaviors of the vehicle-slab track system, a detailed model considering nonlinear subgrade support and initial track state due to track self-weight was developed by Guo *et al.* (2018). The investigation indicated that subgrade settlement results in additional track irregularity, and locally, the contact between the concrete track and the soil subgrade is prone to failure. Moreover, wheel-rail interaction is significantly exacerbated by the track degradation and abnormal responses occur as a result of the unsupported areas. Distributions of interlaminar contact forces in track system vary dramatically due to the combined effect of track deterioration and dynamic load. These may not only intensify the dynamic responses of the coupled system, but also have impacts on the long-term behavior of the track components.

The aim of this research is to study the advantages of utilizing geogrid as reinforcement to

minimize the amount of degradation of ballast under railway track base resting on clayey soil and determine the transmitted stresses and the developed excess pore water pressure in the clay layer due to dynamic load.

2. Laboratory works and model preparation

2.1 Soil and materials used

A brown clayey soil was brought from a site in Baghdad city. Standard tests were performed to determine the physical properties of the soil. Details are given in Table 1. According to the Unified Soil Classification System U.S.C.S, the soil is classified as CL. A consolidation test was performed for soft and stiff clay states according to ASTM 2435 – 96. Table 2 lists the consolidation test results for both states of the clay.

Table 1 Physical properties of clay used

Liquid limit (LL)	46	Clay %, < 0.005 mm	61
Plastic limit (PL)	21	D ₈₅ mm	0.018
Plasticity index	25	D ₆₀ mm	0.0036
Specific gravity (Gs)	2.65	D ₃₀ mm	-
Gravel %, > 4.75 mm	0	D ₁₅ mm	-
Sand %, 0.075-4.75 mm	4	D ₁₀ mm	-
Silt %, 0.005-0.075 mm	35	Activity	0.41

Table 2 Consolidation test results for soft and stiff clay

Parameter	Soft state	Stiff state
Undrained shear strength, C _u	20-25 kN/m ²	≈ 50 kN/m ²
Initial void ratio, e _o	0.61	0.38
Dry unit weight, γ _{dry}	16.6	19.3
Saturated unit weight, γ _{sat}	21.6	23.4
Compression index, C _c	0.18	0.1
Expansion index, C _r	0.1	0.05

Table 3 Ballast particle size characteristics

Parameter	Value	Parameter	Value
D ₆₀	21.59 mm	Coefficient of gradation, C _c	1.07
D ₃₀	20.61 mm	γ _{dry min}	15.21 kN/m ³
D ₁₀	18.35 mm	γ _{dry max}	19.25 kN/m ³
Coefficient of uniformity, C _u	1.18	γ _n	17.83 kN/m ³

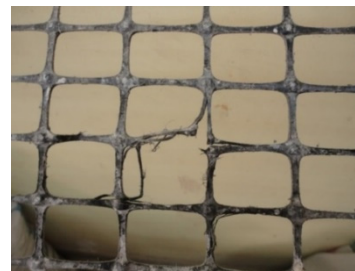
The ballast was obtained from a private crushed stone factory. It was produced as a result of crushing big stones; the ballast is of white color with angular shapes. The effective size, uniformity coefficient and coefficient of gradation are listed in Table 3. The ballast is of uniform size with poorly graded gradation (GP) according to the Unified Soil Classification System.

Geogrid reinforcement

The geogrid used in all tests was manufactured by Tensar type SS2, Fig. 1, its engineering



(a) Before test



(b) Damage in used geogrid reinforcement

Fig. 1 Geogrid reinforcement used in tests

Table 4 Tensar SS2 geogrid specification

Property	Units	
Polymer		Polypropylene
Minimum carbon black (2)	%	2
Roll width	m	4.0
Roll length	m	50
Unit weight	Kg/m ²	0.29
Roll weight	Kg	60
Dimensions		
A _L	mm	28
A _T	mm	40
W _{LR}	mm	3.0
W _{TR}	mm	3.0
t _J	mm	3.8
t _{LR}	mm	1.2
t _{TR}	mm	0.9
Rib shape		Rectangular
Quality Control Strength (longitudinal)		
T _{ult} (3)	kN/m	17.5
Load at 2% strain (3)	kN/m	7.0
Load at 5% strain (3)	kN/m	14.0
Approximate. strain at T _{ult}	%	12.0

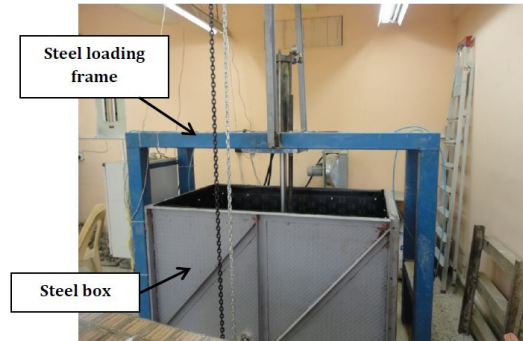


Fig. 2 Steel frame of the loading system

properties are shown in Table 4 as provided by the manufacturing company. The sheet of geogrid was used in multiple tests but was replaced whenever become visibly overstressed or damaged as shown in Fig. 1.

Model tests

Load setup design and manufacturing

To study the response of the railway ballast to track loads on a clay layer, it is necessary to simulate the condition as close as possible to those occurring in the field. To achieve this aim, a special testing apparatus and other accessories are designed and manufactured. The apparatus has the capability of applying different dynamic loads under different frequencies.

The general view of the apparatus is shown in Fig. 2. The apparatus consists of the following:

1. Loading steel frame.
2. Hydraulic loading system.
3. Load spreader beam.
4. Data acquisition.
5. Shaft encoder.
6. Steel container.

Steel loading frame

To support and ensure the verticality of the hydraulic jack used in applying the central concentrated load, a steel frame was designed and constructed as shown in Fig. 2. The steel frame consists mainly of four columns and four beams. Each column and beam are made of steel with square cross section area of (100 mm × 100 mm) and 4 mm thick. The dimensions of the steel frame (length × width × height) are (1700 mm × 700 mm × 1700 mm). To strengthen the steel frame, two vertical steel channels were welded.

Hydraulic loading system

As shown in Fig. 3, the system contains a hydraulic steel tank with a capacity of 70 liters. The tank consists of two holes; the upper one is used to fill the oil and the lower one is for discharge. The tank includes a gear type hydraulic pump with a fixed geometrical volume giving a discharge about 12 liter/min with a maximum pressure of 150 bars. The axis of the pump is connected by a coupling with a three phase electrical rotary motor of 3 hp capacity and 1450 rpm rotation speed. The pump and the motor are fixed in a housing on the upper surface of the tank.

During the rotation of the pump, it sends the hydraulic through a flexible hose to distributional block where there are two directional valves fixed to it, the first one which works in one direction is used as a key to lock the hydraulic in the system or send it back to the tank. This hydraulic valve is connected with another directional valve which controls the moving of the hydraulic cylinder

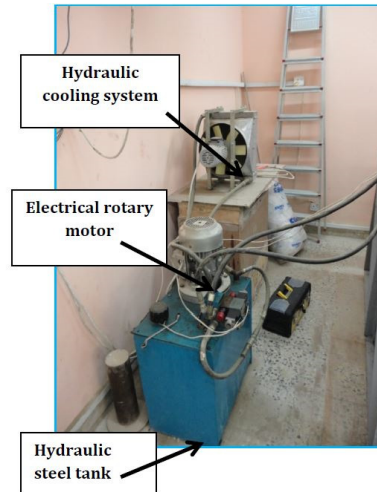


Fig. 3 Hydraulic loading system

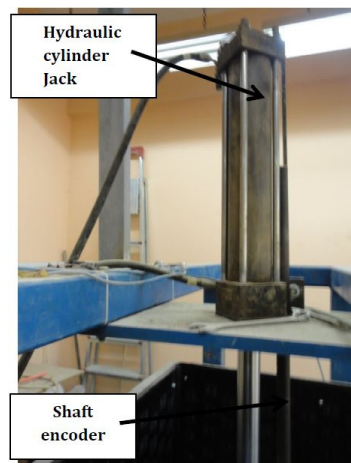


Fig. 4 Hydraulic cylinder jack



Fig. 5 Load spreader beam and Linear Variable Differential Transformers (LVDTs)

jack up and down Fig. 4. The movement of the hydraulic cylinder jack is controlled electrically by a Programmable Logic Control (PLC) through which, the movement (up and down) can be controlled by choosing the hearts that are needed in the control through data acquisition system. The data acquisition system also displays the load magnitude that applied on the rail.

Load spreader beam

An 80 cm × 5 cm × 5 cm solid steel beam was used to apply the load on the track panel as shown in Fig. 5.

The steel container

The tests were carried out in a steel container with a plan dimension of 1.5 m length × 1 m width × 1 m height. Each part of the container is made of steel plate 5 mm thick. The container is made of five well welded parts, one for the base and others for the four sides of the container. The long sides were braced externally by angles at their edges. The base is externally stiffened by three channels of (50 mm web × 25 mm flange).

Data acquisition system

Data acquisition system is used to measure and sense the occurring displacement during the tests, which enable the tester to obtain a huge data of readings in a very short time, moreover it is used to choose the specified frequency used in the test as shown in Fig. 6. The data acquisition system consists of Programmable Logic Controller (PLC) which can be defined as a digital computer used for electro-mechanical automation processes, and it is a high technology processing unit. This type of systems analyzes the data digitally.

PLC device comprises of LCD touch-screen panel is used for viewing the input and output data by simplified ladder logic. This LCD is a touch-screen where accompanied by three- push buttons to lead the operator for commands related for the test, and enable the user to use a simple windows for programming the input requirement and storing the results into the computer for calculation.

The program of Programmable Logic Controller (PLC) is executed repeatedly whenever the controlled system is running and then the data is saved in its memory although the electricity current was turned off.

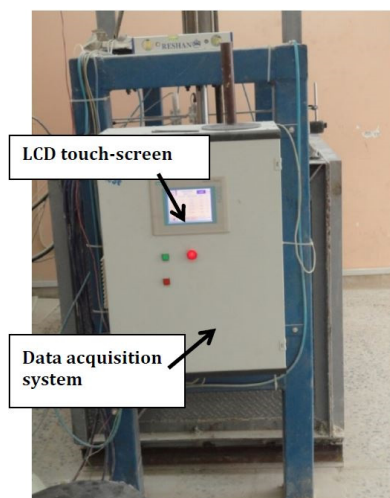


Fig. 6 The data acquisition system



Fig. 7 Earth pressure cells

Shaft encoder

A shaft encoder is an electro-mechanical device used to convert the motion of the shaft to a digital code. The output of incremental encoder supply information of the motion of the shaft which is processed into information such as, displacement, revolution per minute (rpm), speed, and position.

Instrumentation

Displacement transducers (Linear Variable Differential Transformers (LVDTs))

A total of four Linear Variable Differential Transformers (LVDTs) were used to instrument the ends of the track panel as shown in Fig. 5. The (LVDTs) were used, to measure the surface displacement of railroad track to check it with the shaft encoder measurement.

Pressure cells and piezometer

A heavy duty cells Model 3515 Geokon pressures cells are used. They are suitable for railroad applications. Three pressure cells were placed between the clay and ballast right beneath the railroad as shown in Fig. 7. These earth pressure cells have a diameter of 100 mm and a capacity of 0-250 kPa.

Model 3400 Geokon Series Piezometers are used to measure ground water elevations and pore-water pressures in bore holes, embankments, concrete structures, pipe lines, wells etc.

Track panel

A track panel that consists of two rails 80 cm in length and three wooden sleepers (90 cm x 9 cm x 9 cm) was used in the tests as shown in Fig. 8. Fig. 9 shows the dimensions of the rail used in the tests in contrast with the real rail dimensions. The spacing between the rails and the sleepers is 300 mm and 650 mm center to center, respectively.

Model preparation

The construction of the ballast layer starts after three days from the preparation of the soil bed. The ballast is placed carefully on the surface of the soil bed in layers; each layer is not more than 100 mm thick. A predetermined volume of ballast is prepared which is sufficient to create a uniform layer. Each layer is compacted gently by a tamping rod to attain a placement dry unit weight of about 17.83 kN/m³. This placement unit weight corresponds to a relative density of

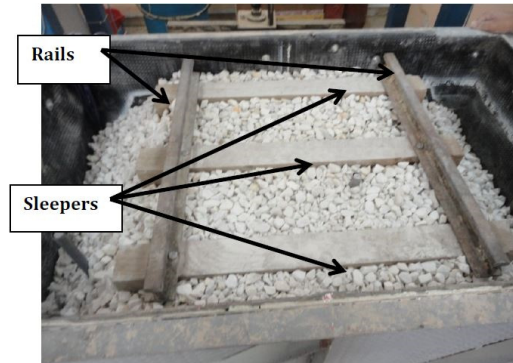


Fig. 8 Track panel

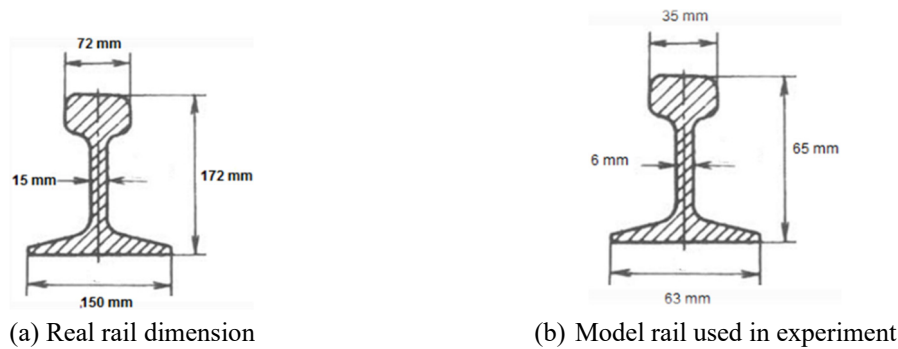


Fig. 9 Dimensions of the rail (Li *et al.* 2016)

about 70%.

A half full-scale railway was constructed for carrying out the tests. Two rails 80 cm in length with three wooden sleepers (90 cm × 9 cm × 9 cm) were used to construct the track panel, Fig. 10. Three values of ballast thicknesses of 20, 30 and 40 cm were used in the tests, each side of the ballast was sloped down on about 2:1 slope. The ballast was overlying 50 cm thickness clay in two states, soft and stiff state. The tests were carried out with and without geogrid reinforcement. Fig. 11 illustrates how the laboratory test sections are constructed.

Test procedure

The test was carried out in a well tied steel box of 1.5 m length × 1 m width × 1 m height, the box was padded with two layers, the first one consists of compressed styropor sheets 5 mm thick and the other one is a rubber 4 mm thick to prevent reflection of waves during the test.

The box was filled with relatively soft clay which was placed in 100 mm layers to ensure the consistency and was compacted by plywood to a depth of 500 mm. After the placement of each layer, it was pressed gently with a wooden tamper in order to remove entrapped air.

The clay material used in the tests has a wet unit weight of 21.6 kN/m³, moisture content of about 30% and a drained shear strength of about 25 kN/m² when it was finally placed in the box in its soft state and of a wet density (23.4 kN/m³), moisture content of about 21% and a drained shear strength about 50 kN/m² when it was finally placed in its stiff state, the liquid limit of the clay was

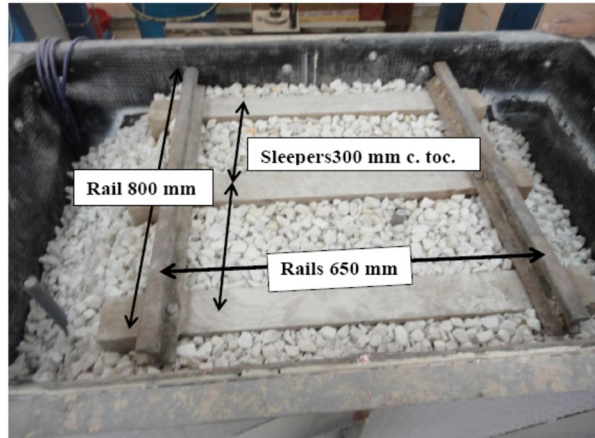


Fig. 10 Track panel dimensions

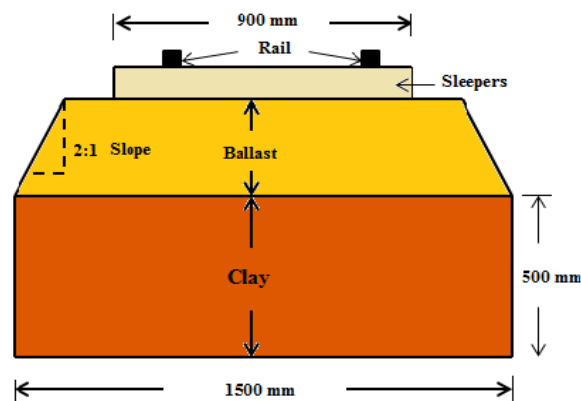


Fig. 11 The laboratory test section

found to be 46% while the plastic limit is 21%.

In the laboratory, ballast was hoisted and placed over the clay layer in the box by using 2 ton manual chain hoists, where the ballast was placed in plastic containers and then the ballast is thrown carefully to allow the ballast to fall into the box in a controlled manner. A predetermined weight of ballast was prepared in accordance with the expected volume and the density used in the tests. The ballast was placed and compacted in 100 mm layers by using a tamping rod to attain a dry unit weight of (17.83 kN/m^3) corresponding to a relative density of about 70% to depths of 200 mm or 300 mm or 400 mm as the test required. The angle of the slope of the ballast was controlled by maintaining alignment with markings on the wall of the box.

During preparation of the ballast layer, the geogrid was laid in predetermined position as specified in the reinforced ballast tests. Then the track panel was placed into its particular position via using the manual chain hoists and a good seating on the surface of the ballast was achieved by tamping it carefully. Special care was given to the leveling of the track panel and sleeper at the position where the rail must be placed. Additional amount of ballast was then added between and at ends of the sleepers to achieve restraint. Stress transmitted and excess pore water pressure

developing from the applied load were recorded by three pressure cells installed on the clay surface and a piezometer installed at 50 mm depth in the clay layer, they were placed at specific locations to measure the stresses transmitted by the ballast to the clay layer. The traffic loading simulation on the sleepers was executed by applying rectified sine wave loading. This type of loading was suggested by Awoleye (1993). It simulates a running of train over three sleepers in which 50% of the wheel load is transmitted to the middle sleeper and 25% of the wheel load on both outer sleepers. The frequency of loading in the test was up to 2 Hz. This frequency is considered low when it is compared to the usual frequency in the track which is approximately 8–10 Hz. This frequency was however associated with the pressure and flow capacity of the hydraulic loading system. The effect of applying geogrid reinforcement was examined by the comparison of settlement magnitude, the pressure and pore water pressure developed in the clay layer performed in various tests with and without geogrid in the ballast layer. The tests with sand drains had been carried out in the same way of the other tests, with installing the sand drains before the ballast placement.

Testing program

Table 5 lists the experimental tests that are carried out. To facilitate the discussion of the results, tests are given symbolic names; these names will be adopted under the variables in the experiments as shown in Table 5.

Table 5 Tests identification for models on soft clay

Test name identification	Ballast thickness, cm	Load amplitude, ton	Load frequency, Hz	No. of layers	Layer position (h/T)
T30 A2 f1 NL0	30	2	1	0	-
T30 A2 f1 NL1-0.25	30	2	1	1	0.25
T30 A2 f1 NL1-0.5	30	2	1	1	0.5
T30 A2 f1.5 NL0	30	2	1.5	0	-
T30 A2 f1.5 NL1-0.25	30	2	1.5	1	0.25
T30 A2 f1.5 NL1-0.5	30	2	1.5	1	0.5
T30 A2 f2 NL0	30	2	2	0	-
T30 A2 f2 NL1-0.25	30	2	2	1	0.25
T30 A2 f2 NL1-0.5	30	2	2	1	0.5
T30 A1 f1 NL0	30	1	1	0	-

where:

- T: ballast layer thickness for soft clay tests, cm,
- ST: ballast layer thickness for stiff clay tests, cm,
- DT: ballast layer thickness with sand drains tests, cm,
- A: load amplitude, ton,
- F: load frequency, Hz,
- NL: number of geogrid layers and geogrid layer position (h/T) in ballast layer, and
- h: position of geogrid layer in ballast layer from the upper surface of the clay layer.

Cumulative vertical settlement

Effect of load frequency on the cumulative vertical settlement

Figs. 12 to 20 show the typical relationship of settlement versus number of cycles for different load frequencies. As observed from these figures, almost in ballast thickness of 20 cm at low load amplitude, the settlement at high load frequency is more than at low load frequency and the existence of geogrid reduces the effect of load frequency on the settlement, this may be due to the contribution of reinforcement layer in absorbing and attenuation of the load waves when it is transmitted through the reinforcement to the lower base layer. On the other hand, there is no clear effect of load frequency at high load amplitude for ballast thickness of 20 cm and for all load amplitudes for ballast thickness of 30 cm.

The geogrid employs the effect of interlocking between granular particles. The granular particles will penetrate the apertures of geogrid and locked between the strands of geogrid. This mechanism of immobilization of the reinforced particles gives a strong shear resistance, which will reduce the lateral movement and increase the bearing capacity of the base layer.

Figs. 21 to 29 show the relationship between the load frequency and the settlement ratio. As seen in these figures, the effect of load frequency on the settlement ratio is almost constant after 500 cycles. This is due to that the total settlement after 500 cycles, almost reached its peak value, which means that the ballast particles become very close to each other, so the load frequency will be less effective for the high contact particles forces.

The figures show that in general for reinforced cases, the effect of load frequency on the settlement ratio is very small ranging between 0.5-2 percent, in contrast to the unreinforced case. These results are consistent with those of Lekarp *et al.* (2000) who reported that “the frequency and load duration have little or no significant effect on the resilient modulus for granular materials”. However, they also mentioned that “the resilient modulus may decrease with increase in frequency in an undrained condition”. The resilient modulus as defined by Seed *et al.* (1962) is the repeated deviator stress divided by the recoverable (resilient) axial strain during unloading in a triaxial test.

Placement of geogrid layer or layers in or at the bottom of the base course allows for shear interaction to develop between the aggregate and the geogrid, as the base attempts to spread laterally. Shear load is transmitted from the base aggregate to the geogrid and places the geogrid in tension. The relatively high stiffness of the geogrid acts to retard the development of lateral tensile strain in the base adjacent to the geogrid. Lower lateral strain in the base results in less vertical deformation of the railway surface. Hence, the first mechanism of reinforcement corresponds to direct prevention of lateral spreading of the base aggregate.

The particle breakage contributes to the generation of fines which in the long-term accumulates and decreases the permeability of ballast that can eventually cause undrained failure of track during and after heavy rainfall.

However, the geogrid reinforcement reduces the extent of particle breakage. The reduction in particle breakage may be attributed to the interlocking of particles within the geogrid apertures that subsequently increases the confining pressure on ballast (Hussaini 2013).

As seen from the figures, the effect of load amplitude on the settlement of the composite in the beginning of the tests was almost negligible with reinforced and unreinforced ballast layer, so the settlement ratio difference was too small between them while it was increased with increasing the number of cycles. This is likely to be due to ineffective interlocking between the ballast particles and the geogrid at the beginning of the test.

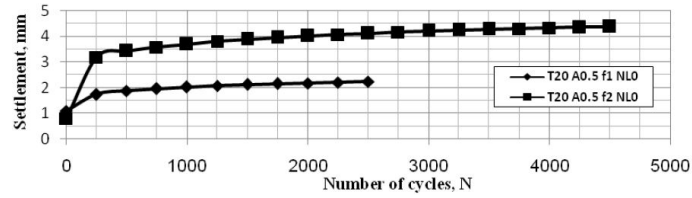


Fig. 12 Settlement versus number of cycles for different load frequencies with ballast thickness 20 cm, amplitude 0.5 ton and without reinforcement

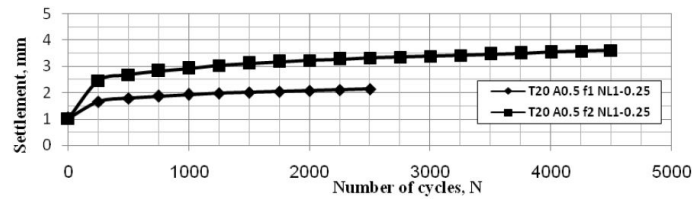


Fig. 13 Settlement versus number of cycles for different load frequencies with ballast thickness 20 cm, amplitude 0.5 ton and with one layer of reinforcement $h/T = 0.25$

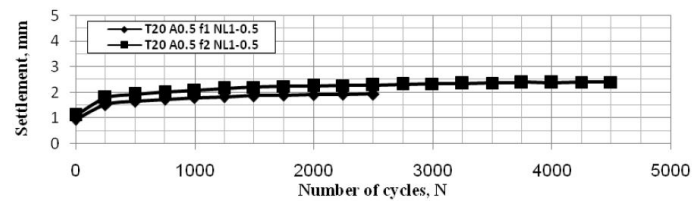


Fig. 14 Settlement versus number of cycles for different load frequencies with ballast thickness 20 cm, amplitude 0.5 ton and with one layer of reinforcement $h/T = 0.5$

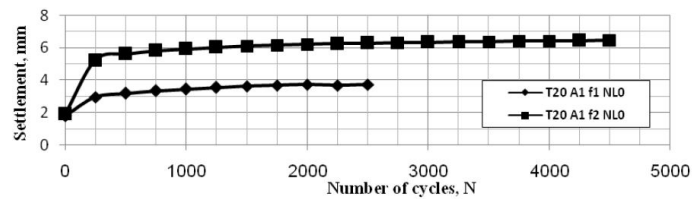


Fig. 15 Settlement versus number of cycles for different load frequencies with ballast thickness 20 cm, amplitude 1 ton and without reinforcement

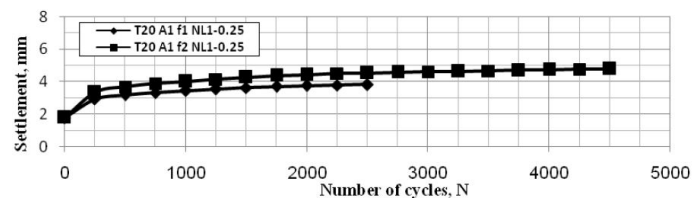


Fig. 16 Settlement versus number of cycles for different load frequencies with ballast thickness 20 cm, amplitude 1 ton and with one layer of reinforcement $h/T = 0.25$

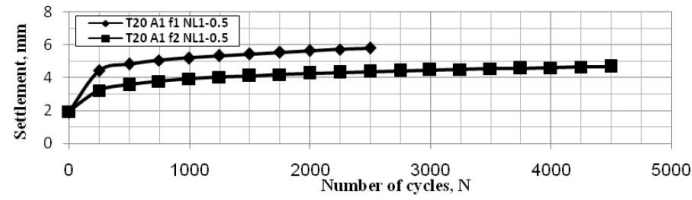


Fig. 17 Settlement versus number of cycles for different load frequencies with ballast thickness 20 cm, amplitude 1 ton and with one layer of reinforcement $h/T = 0.5$

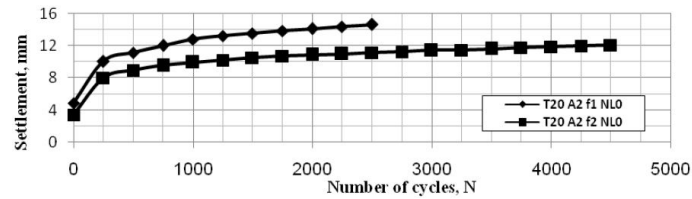


Fig. 18 Settlement versus number of cycles for different load frequencies with ballast thickness 20 cm, amplitude 2 ton and without reinforcement

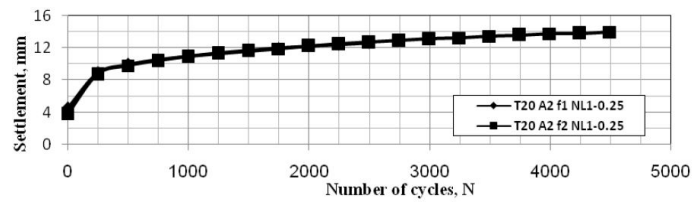


Fig. 19 Settlement versus number of cycles for different load frequencies with ballast thickness 20 cm, amplitude 2 ton and with one layer of reinforcement $h/T = 0.25$

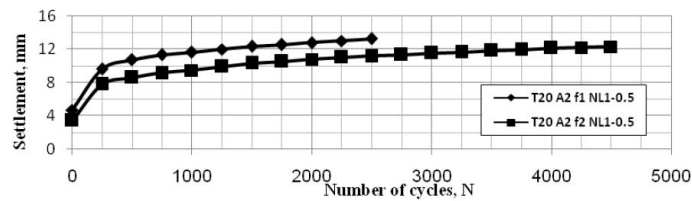


Fig. 20 Settlement versus number of cycles for different load frequencies with ballast thickness 20 cm, amplitude 2 ton and with one layer of reinforcement $h/T = 0.5$

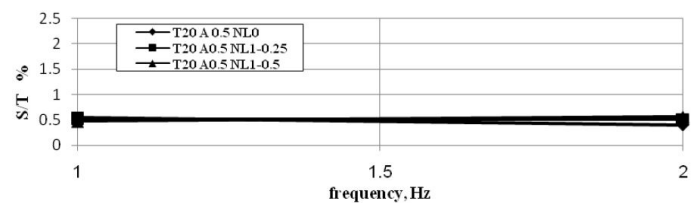


Fig. 21 Effect of load frequency on the settlement ratio at the beginning of the test, with ballast thickness 20 cm, amplitude 0.5 ton

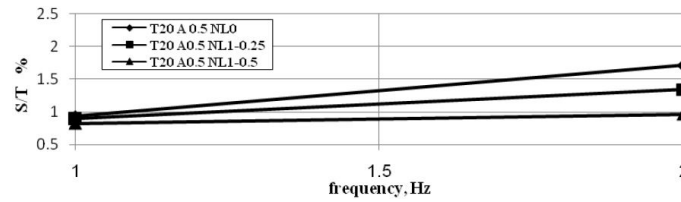


Fig. 22 Effect of load frequency on the settlement ratio with ballast thickness 20 cm, amplitude 0.5 ton after 500 cycles

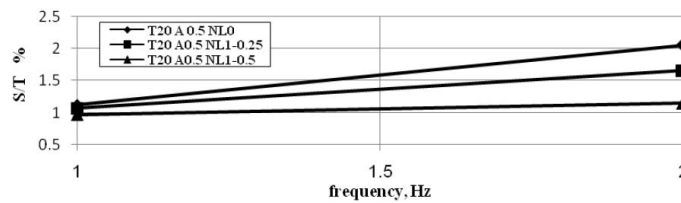


Fig. 23 Effect of load frequency on the settlement ratio with ballast thickness 20 cm, amplitude 0.5 ton at the end of the test (2500 cycles)

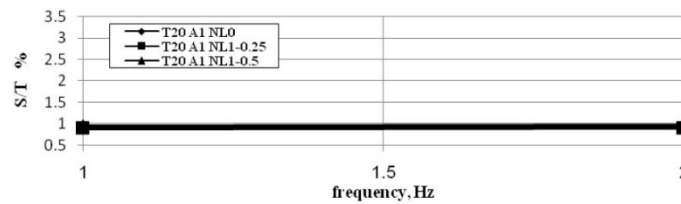


Fig. 24 Effect of load frequency on the settlement ratio at the beginning of the test, with ballast thickness 20 cm, amplitude 1 ton

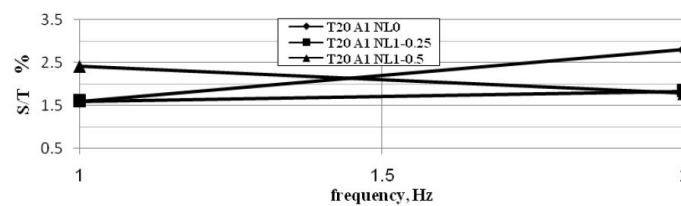


Fig. 25 Effect of load frequency on the settlement ratio with ballast thickness 20 cm, amplitude 1 ton after 500 cycles

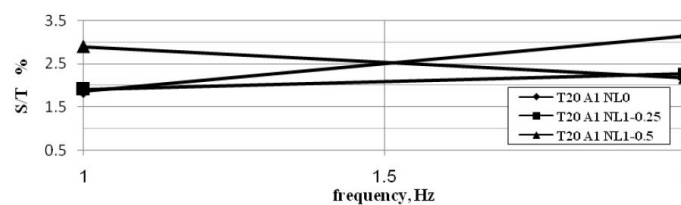


Fig. 26 Effect of load frequency on the settlement ratio with ballast thickness 20 cm, amplitude 1 ton at the end of the test (2500 cycles)

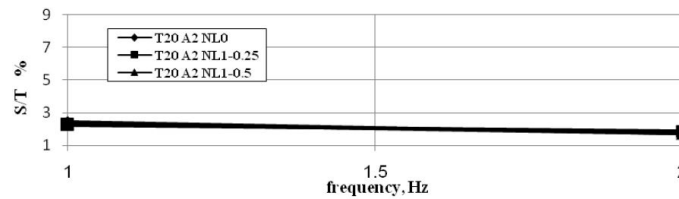


Fig. 27 Effect of load frequency on the settlement ratio at the beginning of the test, with ballast thickness 20 cm, amplitude 2 ton

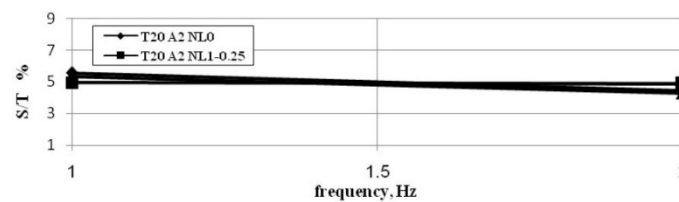


Fig. 28 Effect of load frequency on the settlement ratio with ballast thickness 20 cm, amplitude 2 ton after 500 cycles

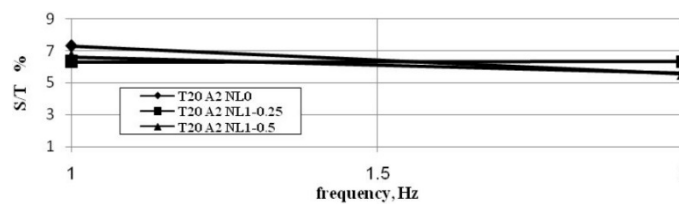


Fig. 29 Effect of load frequency on the settlement ratio with ballast thickness 20 cm, amplitude 2 ton at the end of the test (2500 cycles)

Effect of load frequency on the transmitted average maximum vertical stress and generated pore water pressure

The effect of load frequency is explained in Figs. 30 to 32. From the figures, it can be observed that for ballast thickness 20 cm, the average maximum vertical stress and pore water pressure increased by increasing the load frequency in both reinforced and unreinforced ballast and for all load amplitudes, except for unreinforced ballast at load amplitude 2 tons where the opposite was observed. This may happen due to that at 2-ton load amplitude, the clay layer failed causing a reduction in its stiffness and a reduction in the carrying capacity to the applied stresses. For the ballast thickness of 30 cm at load amplitude of 0.5 and 1 ton, the figures show that there is an increase in the average maximum vertical stress and in pore water pressure by increasing the frequency from 1 to 1.5 Hz, but there is a decrease in the stresses at load frequency 2 Hz for reinforced and unreinforced ballast. On the other hand, it was observed that at load amplitude of 2 tons, there is almost a reduction in stresses for reinforced and unreinforced ballast layer.

Majeed *et al.* (2018) concluded that the effect of load frequency on the surface pressure of subgrade layer is higher when the load amplitude is higher and the subgrade degree of saturation is lower. The higher load frequency result in higher generated stresses at the subgrade layer surface and in soil mass.

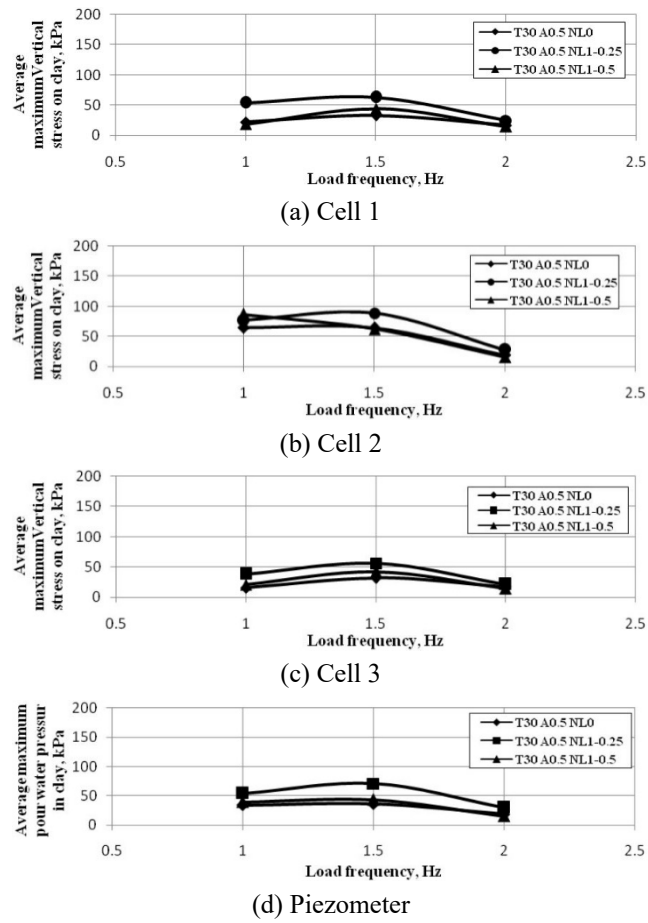


Fig. 30 Effect of load frequency on average maximum vertical stress and pour water pressure with soft clay, ballast thickness 30 cm, amplitude 0.5 ton

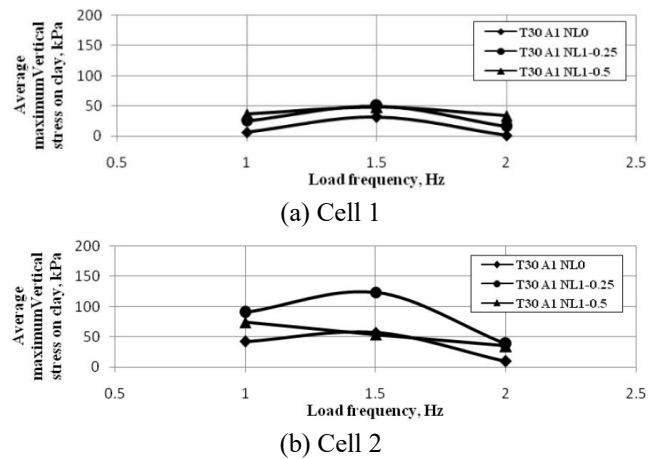
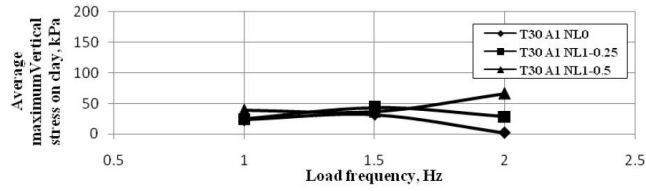
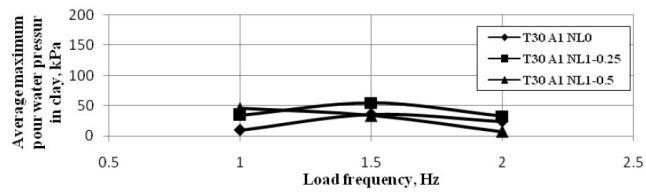


Fig. 31 Effect of load frequency on average maximum vertical stress and pour water pressure with soft clay, ballast thickness 30 cm, amplitude 1 ton

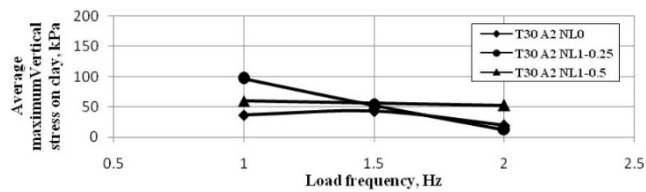


(c) Cell 3

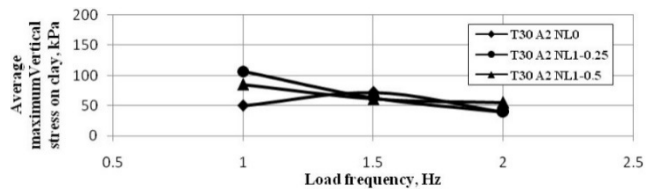


(d) Piezometer

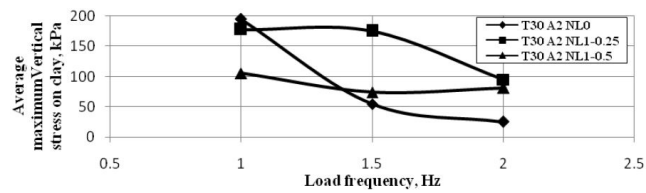
Fig. 31 Continued



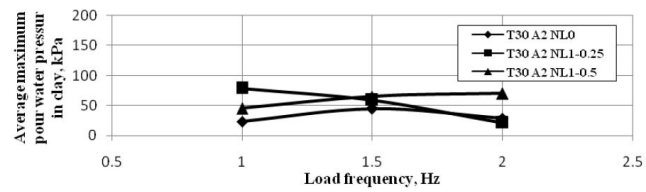
(a) Cell 1



(b) Cell 2



(c) Cell 3



(d) Piezometer

Fig. 32 Effect of load frequency on average maximum vertical stress and pore water pressure with soft clay, ballast thickness 30 cm, amplitude 2 ton

Table 6 Material properties used in the numerical analysis

Parameter	Clay	Ballast	Sleeper (timber)	Rail (steel)
Material model	Hardening soil	Mohr-Coulomb	Linear elastic	
Drainage type	Undrained		Drained	
Unit weight kN/m ³	19.5	17.83	9	78.5
Modulus of elasticity kN/m ²		110×10 ³	7.2×10 ⁶	205×10 ⁶
Cohesion S _{u,c}	25	1	-	-
Friction angle (phi)	0	45°	-	-
Dilatancy angle, Ψ	0	10	-	-
Poison's ratio, ν	0.449	0.35	0.3	0.28
e _{initial}	0.61	0.7	0.5	0.5
Compression index, C _c	0.18	-	-	-
Swelling index C _s	0.1	-	-	-
Geogrid normal elastic stiffness EA kN/m		600		

Finite element analysis for track model

An application of numerical analysis was made using the finite element program PLAXIS 3D 2013 in order to verify the numerical model and for the comparison between theoretical and experimental results is carried out. Table 6 lists the material properties used in the analysis.

PLAXIS 3D is a three dimensional finite element program, developed for the analysis of deformation, stability and groundwater flow in geotechnical engineering. It is a suite of finite element programs that is used for geotechnical engineering and design. PLAXIS provides a tool for practical analysis to be used by geotechnical engineers who are not necessarily numerical specialists.

The calculation consists of three phases except the initial phase for generating the initial stresses with active groundwater table. The process of setting the ballast was chosen in phase one. Phase two was to simulate the elements of the railway track (sleepers and rail). The dynamic load was selected in phase three to consider settlement and stresses in the soil.

To simulate the plane strain boundary condition (y direction) as in the test model, two plates were constructed in the xz plane at ballast cross section at the minimum and maximum y direction to prevent the ballast movement in this direction. Interface surface between the plate and the ballast was added to allow ballast movement in x and z direction.

The ballast is assumed to follow a Mohr-Coulomb failure criterion. The rail and sleepers are modeled as linear elastic, non-yielding behavior is expected for sleepers and rails and a high magnitude of stiffness of these materials is assumed in comparison to those of the ballast. Clayey soils are modeled as a hardening undrained soil without considering any time-dependent behavior, such as consolidation. The geogrid was modeled as an elastic material.

Results of comparison models and discussion

The comparison will be carried out for the model tests, T20 A2 f1 NL0, T20 A2 f1 NL1-0.25, T30 A1 f1 NL0, T30 A2 f1 NL1-0.25, T30 A2 f2 NL0, and T30 A2 f2 NL1-0.25, (Where T: ballast layer thickness cm, A: load amplitude (ton), f: load frequency (Hz), and NL: number of geogrid

layers and layer position).

Figs. 33 to 37 present the settlement versus number of cycles relationship for experimental and numerical results.

From the figures, it can be observed that, both experimental and numerical results have the same behavior. For unreinforced case, it was observed that the experimental results at the beginning show higher readings than the numerical ones, but after a number of cycles ranging from (750) to (2500) cycles the numerical results show higher readings. At the same time, it can be observed that, for reinforced case the experimental results are always higher than the numerical.

Fattah *et al.* (2020a) concluded that the improvement in settlement for soft clay model increases by increasing the speed more than 30 km/hr. For unreinforced models with soft clay layer, at low speed (30 km/hr), about 100 % of the total settlement appears in the clay layer. For stiff clay layer model, there is no effect of reinforcement on the behavior of settlement.

The effect of load amplitude on the settlement of the composite in the beginning of the tests was almost negligible with reinforced and unreinforced ballast layers, so the settlement ratio difference was small between them, while it increased with an increase in the number of cycles (Fattah *et al.* 2020b).

Figs. 24 to 28 show the developed pressure and pore water pressure with number of cycles

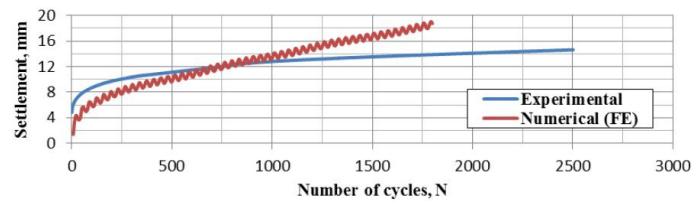


Fig. 33 Comparison between the measured and predicted settlement versus number of cycles for test T20 A2 f1 NL0

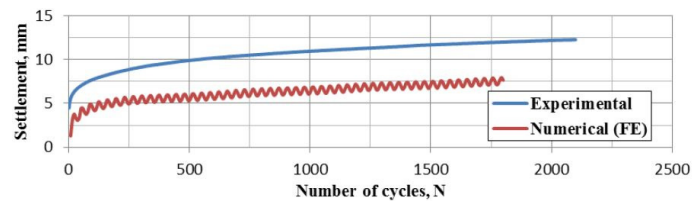


Fig. 34 Comparison between the measured and predicted settlement versus number of cycles for test T20 A2 f1 NL1-0.25

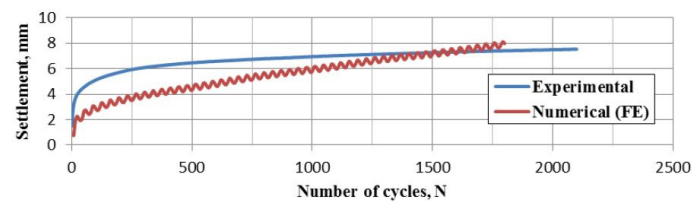


Fig. 35 Comparison between the measured and predicted settlement versus number of cycles for test T30 A1 f1 NL0

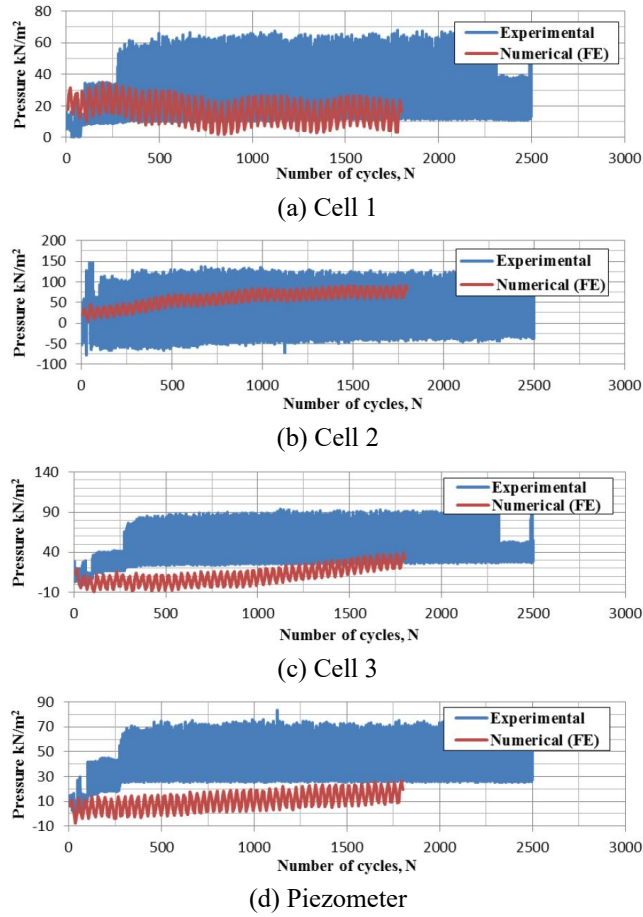


Fig. 36 Comparison between the measured and predicted pressure with number of cycles for test T20 A2 f1 NL0

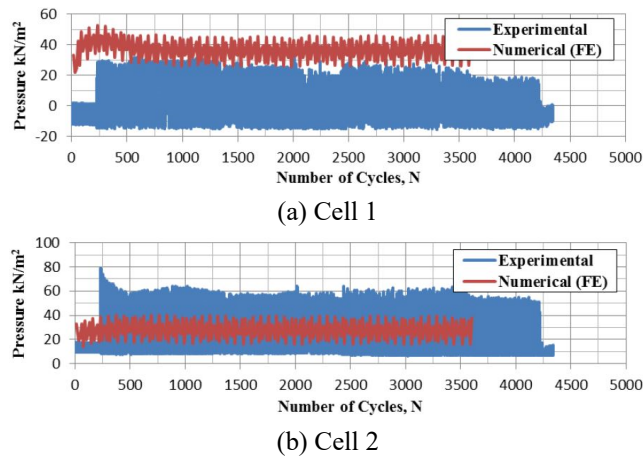
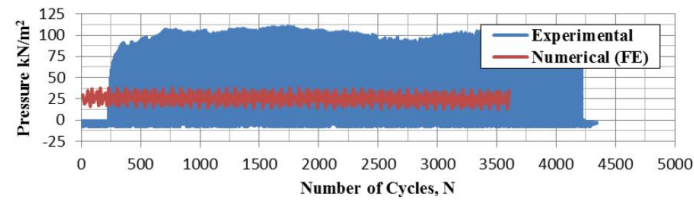
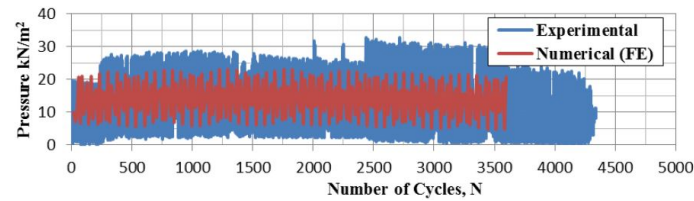


Fig. 37 Comparison between the measured and predicted pressure with number of cycles for test T30 A2 f2 NL1-0.25



(c) Cell 3



(d) Piezometer

Fig. 37 Continued

relationship for experimental and numerical results. From the figures, it can be observed that, the experimental tests almost have higher readings and a wider range of readings.

Inclusion of reinforcement will redistribute the applied load to a wider area, thus minimizing stress concentration and achieving a more uniform stress distribution. Placement of a geogrid layer or layers in or at the bottom of the ballast course allows for shear interaction to develop between the ballast and the geogrid, as the base attempts to spread laterally. Fig. 38 presents contour lines of the vertical displacement along that section for the test model T30 A2 f1 NL1-0.25. Fig. 39 shows contour lines of the total vertical stress along a horizontal section at clay layer surface.

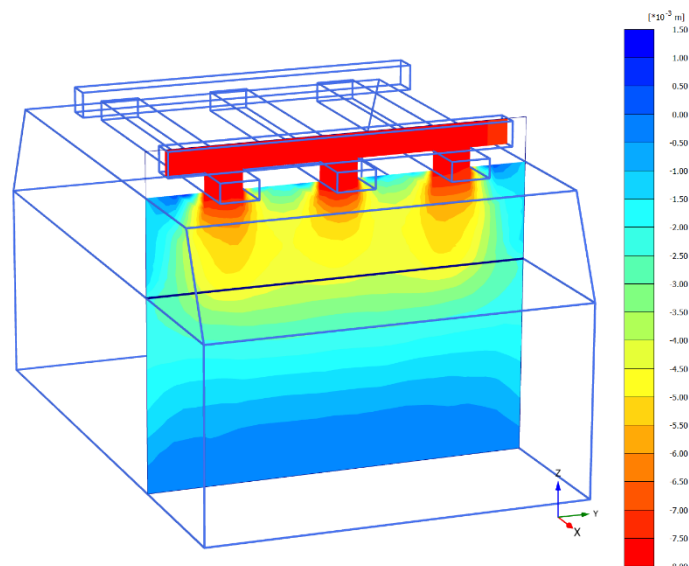


Fig. 38 Displacement in z direction, vertical section at the end of phase three for the test model T30 A2 f1 NL1-0.25

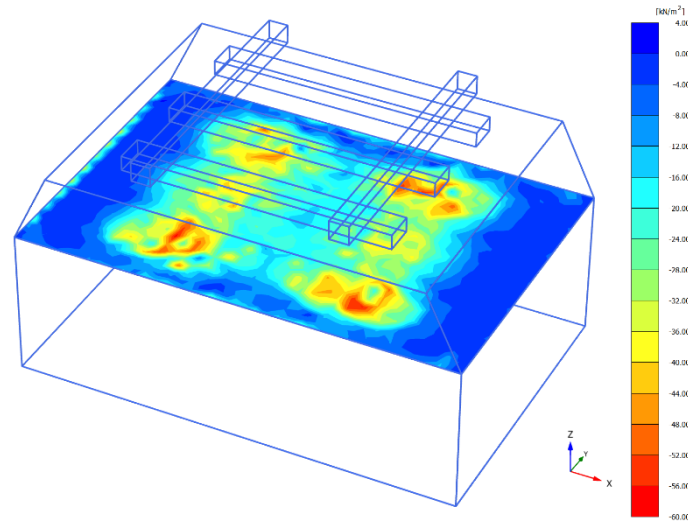


Fig. 39 Total stresses (kPa) in z direction, horizontal section, at the end of phase three for the test model T30 A2 f1 NL1-0.25

3. Conclusions

This paper investigated the influences of load amplitude, load frequency, geogrid position, number of geogrid layers, thickness of ballast layer, clay stiffness, installation of sand drains in the clay layer and induced strain in geogrid on the basis of experimental tests. A series of experimental model tests based on an approximate half scale for general rail track engineering practice was used to study the behavior with and without the inclusion of a geogrid in the ballast layer subjected to dynamic loading. A series of full scale railway track simulations is analyzed by the finite element method using the program PLAXS 3D 2013.

- (1) The effect of load frequency on the settlement ratio is almost constant after 500 cycles. This is due to that the total settlement after 500 cycles, almost reached its peak value, which means that the ballast particles become very close to each other, so the load frequency will be less effective for the high contact particles forces. In general for reinforced cases, the effect of load frequency on the settlement ratio is very small ranging between 0.5-2 percent, in contrast to the unreinforced case.
- (2) For most cases and in all stages of the tests at low load amplitude (0.5 ton), there is almost equal settlement for reinforced and unreinforced ballast layer. The effect of load amplitude on the settlement of the composite was almost negligible in the beginning of the tests with reinforced and unreinforced ballast layer, so the settlement ratio (S/T) (which is the cumulative settlement (S) divided by ballast thickness (T)) difference was too small between them while it was increased with increasing the number of cycles.
- (3) The initial settlement ratio for 2 ton amplitude varied between 1-2% while for 0.5 and 1 ton amplitude, it varied between 0.5-1 percent, this observation includes reinforced and unreinforced ballast. There was little difference in the effect of load amplitude on the settlement ratio between reinforced and unreinforced ballast with stiff clay at the beginning of the test especially at low load amplitude. While at 500 cycles and more, especially at

high load amplitude, the settlement ratio was lower for unreinforced ballast than the reinforced.

- (4) There is very little effect of the geogrid position and number of geogrid layers as well as the existing of the geogrid itself on the magnitude of initial settlement as it is nearly equal to that of unreinforced ballast.
- (5) The transmitted average vertical stress, for ballast thickness 30 cm and 40 cm, increased with increasing the load amplitude regardless the ballast reinforcement, for both soft and stiff clay. There is no significant effect of the geogrid position on the transmitted stresses.
- (6) The values of soil pressure and pore water pressure in case of 20 cm ballast thickness are higher than those of 30 cm and 40 cm. This means that the ballast attenuates the induced waves. The soil pressure as well as pore water pressure for reinforced and unreinforced ballast, are higher in stiff clay than in soft clay. The average maximum vertical stress and pore water pressure increased by increasing the load frequency in both reinforced and unreinforced ballast and for all load amplitudes.
- (7) Both experimental and numerical results have the same behavior. For unreinforced case, it was observed that the experimental results at the beginning show higher readings than the numerical ones, but after a number of cycles ranging from 750 to 2500 cycles, the numerical results show higher readings.

References

- Aikawa, A. (2015), "Research on vertical natural vibration characteristics of gravel aggregate in ballasted track", *Quarterly Report of RTRI*, **56**(1), 26-32. <https://doi.org/10.2219/rtrigr.56.26>
- ASTM D 2435-96 (1996), Standard Test Method for One-Dimensional Consolidation Properties of Soils, Reprinted from the Annual Book of ASTM Standards, Vol. 4, No. 8, West Conshohocken, PA, USA.
- Awolaye, E.O.A. (1993), "Ballast type - Ballast Life Predictions", Derby, British Rail Research LR CES 122, October 1993.
- Chen, C. (2013), "Discrete element modelling of geogrid-reinforced railway ballast and track transition zones", Ph.D. Thesis; University of Nottingham, UK.
- Connolly, D., Giannopoulos, A. and Forde, M.C. (2013), "Numerical modelling of ground borne vibrations from high speed rail lines on embankments", *Soil Dyn. Earthq. Eng.*, **46**, 13-19. <https://doi.org/10.1016/j.soildyn.2012.12.003>
- Fattah, M.Y., Mahmood, M.R. and Aswad, M.F. (2017), "Experimental and numerical behavior of railway track over geogrid reinforced ballast underlain by soft clay", In: *Recent Developments in Railway Track and Transportation Engineering, Sustainable Civil Infrastructures*. https://doi.org/10.1007/978-3-319-61627-8_1
- Fattah, M.Y., Mahmood, M.R. and Aswad, M.F. (2019), "Stress distribution from railway track over geogrid reinforced ballast underlain by clay", *Earthq. Eng. Eng. Vib.*, **18**(1), 77-93. <https://doi.org/10.1007/s11803-019-0491-z>
- Fattah, M.Y., Mahmood, M.R. and Aswad, M.F. (2020a), "Effect of track speed on the behavior of railway track ballast system underlain by clay", *Proceedings of IOP Conference Series: Materials Science and Engineering*, **737**, 012094. <https://doi.org/10.1088/1757-899X/737/1/012114>
- Fattah, M.Y., Mahmood, M.R. and Aswad, M.F. (2020b), "Settlement of railway track on reinforced ballast overlain by clayey", *J. Transport. Logistics*, **5**(2). <https://doi.org/10.26650/JTL.2020.0014>
- Gao, H. (2013), "A 3D dynamic train-track interaction model to study track performance under trains running at critical speed", Master of Science Thesis; Department of Civil and Environmental Engineering, The Pennsylvania State University, PA, USA.
- Guo, Y., Zhai, W. and Sun, Y. (2018), "A mechanical model of vehicle-slab track coupled system with

- differential subgrade settlement”, *Struct. Eng. Mech., Int. J.*, **66**(1), 15-25.
<https://doi.org/10.12989/sem.2018.66.1.015>
- Hayano, K., Ishii, K. and Muramoto, K. (2013), “Effects of Ballast Thickness and Tie-tamper Repair on Settlement Characteristics of Railway Ballasted Tracks”, *Proceedings of the 18th International Conference on Soil Mechanics and Geotechnical Engineering*, Paris, France, September, pp. 1275-1282.
- Hussaini, S.K.K. (2013), “An Experimental Study on the Deformation Behavior of Geosynthetically Reinforced Ballast”, Ph.D. Thesis; University of Wollongong, Australia.
- Krylov, V.V. (1995), “Generation of ground vibrations by superfast trains”, *Appl. Acoust.*, **44**(2), 149-164.
[https://doi.org/10.1016/0003-682X\(95\)91370-I](https://doi.org/10.1016/0003-682X(95)91370-I)
- Lekarp, F., Isacsson, U. and Dawson, A. (2000), “State of the art. I: Resilient response of unbound aggregates”, *J. Transport. Eng.*, **126**(1), 66-75. [https://doi.org/10.1061/\(ASCE\)0733-947X\(2000\)126:1\(66\)](https://doi.org/10.1061/(ASCE)0733-947X(2000)126:1(66))
- Leshchinsky, B. and Ling, H.I. (2013), “Numerical modeling of behavior of railway ballasted structure with geocell confinement”, *Geotext. Geomembr. J.*, **36**, 33-43.
<https://doi.org/10.1016/j.geotexmem.2012.10.006>
- Li, D., Hyslip, J., Sussmann, T. and Chrismer, S. (2016), *Railway Geotechnics*, (E-book), Taylor and Francis Group, LLC.
- Majeed, Q.G., Fattah, M.Y. and Joni, H.H. (2018), “Effect of Load Frequency on the Subgrade Layer Stresses beneath Railways”, *Int. J. Civil Eng. Technol. (IJCIET)*, **9**(11), 838-852.
- Nguyen, K., Goicolea, J.M. and Galbadón, F. (2011), “Dynamic Effect of High Speed Railway Traffic Loads on the Ballast Track Settlement”, Group of Computational
- Profillidis, V.A. (2000), *Railway Engineering*, Ashgate Publishing Limited, Aldershot, UK.
- Seed, H.B., Chan, C.K. and Lee, C.E. (1962), “Resilience characteristics of subgrade soils and their relation to fatigue failures in asphalt pavements”, *Proceedings of International Conference on the Structural Design of Asphalt Pavements*, Ann Arbor, MI, USA, pp. 611-636.
- Selig, E.T. and Waters, J.M. (1994), *Track Geotechnology and Substructure Management*, (1st Ed.), Thomas Telford Publications.
- Sowmiya, L.S., Shahu, J.T. and Gupta, K.K. (2011), “Railway tracks on clayey subgrade reinforced with geosynthetics”, *Proceedings of Indian Geotechnical Conference*, Kochi, India, December, pp. 529-532.
- Wayne, M., Fraser, I., Reall, B. and Kwon, J. (2013), “Performance Verification of a Geogrid Mechanically Stabilized Layer”, *Proceedings of the 18th International Conference on Soil Mechanics and Geotechnical Engineering*, Paris, France, September, pp. 1381-1384.